Journal of Neuropathology and Experimental Neurology

Vol. 60, No. 8
August, 2001
pp. 759–767

Oxidative Damage Is the Earliest Event in Alzheimer Disease

AKIHIKO NUNOMURA, MD, PHD, GEORGE PERRY, PHD, GJUMRAKCH ALIEV, MD, PHD, KEISUKE HIRAI, PHD, ATSUSHI TAKEDA, MD, PHD, ELIZABETH K. BALRAJ, MD, PAUL K. JONES, PHD, HOSSEIN GHANBARI, PHD, TAKAFUMI WATAYA, MD, SHUN SHIMOHAMA, MD, PHD, SHIGERU CHIBA, MD, PHD, CRAIG S. ATWOOD, PHD, ROBERT B. PETERSEN, PHD, AND MARK A. SMITH, PHD

Abstract. Recently, we demonstrated a significant increase of an oxidized nucleoside derived from RNA, 8-hydroxyguanosine (8OHG), and an oxidized amino acid, nitrotyrosine in vulnerable neurons of patients with Alzheimer disease (AD). To determine whether oxidative damage is an early- or end-stage event in the process of neurodegeneration in AD, we investigated the relationship between neuronal 8OHG and nitrotyrosine and histological and clinical variables, i.e. amyloid-β (Aβ) plaques and neurofibrillary tangles (NFT), as well as duration of dementia and apolipoprotein E (ApoE) genotype. Our findings show that oxidative damage is quantitatively greatest early in the disease and reduces with disease progression. Surprisingly, we found that increases in Aβ deposition are associated with decreased oxidative damage. These relationships are more significant in ApoE ϵ4 carriers. Moreover, neurons with NFT show a 40%–56% decrease in relative 8OHG levels compared with neurons free of NFT. Our observations indicate that increased oxidative damage is an early event in AD that decreases with disease progression and lesion formation. These findings suggest that AD is associated with compensatory changes that reduce damage from reactive oxygen.

Key Words: Alzheimer disease; Amyloid β; Apolipoprotein E; 8-hydroxyguanosine; Neurofibrillary tangle; Nitrotyrosine; Oxidative stress.

INTRODUCTION

Several studies have now established the association of neuronal oxidative stress with Alzheimer disease (AD) (1, 2). This stress is manifested by damage to proteins (3–5), lipids (6, 7), and nucleic acids, i.e. nuclear and mitochondrial DNA (8, 9) as well as RNA (10). Apolipoprotein E (ApoE) ϵ4 allele (corresponding protein, ApoE4), a major risk factor for AD, is associated with oxidative damage in vitro (11), in transgenic models (12), and in brain tissue of cases of AD (7, 13, 14). Nevertheless, it is still controversial whether oxidative stress plays an early role in the disease, or alternatively, is secondary to the histopathological changes in AD, amyloid-β (Aβ) deposits and neurofibrillary tangles (NFT). Although in vitro studies support an important role for Aβ in oxidative balance, some of them argue Aβ is the cause (15, 16), while others argue Aβ is the result (17–19) of oxidative stress.

In this study, we address the chronological issue of oxidative stress in a series of cases of AD with different duration of disease by examining the levels of 8-hydroxyguanosine (8OHG), an oxidized nucleoside derived from RNA, and nitrotyrosine, a protein modification. Our analysis focused on oxidative damage to RNA and a noncrosslink protein adduct, because there is no evidence that such modifications are accumulated. This means that their levels more accurately reflect steady-state balance rather than the history of oxidative damage, as often happens for oxidative crosslink modifications to protein (20). Evaluation of relative levels of these oxidative markers in vulnerable neurons in cases of AD with various densities of histopathology enabled us to investigate the relationship between oxidative stress, histological alterations, disease duration, and ApoE genotype in AD. Our findings indicate that oxidative damage to neuronal RNA and protein is an early event in AD pathogenesis, in agreement with our recent study in Down syndrome where we found that neuronal oxidative stress precedes Aβ deposition (21). Surprisingly, levels of both RNA and protein oxidation decrease with duration of disease and with increased histopathology. These findings suggest that the histopathology of AD is linked to compensatory cellular changes that reduce oxidative stress.

MATERIALS AND METHODS

Tissue

Brain tissue was obtained at autopsy from 22 clinically and pathologically confirmed cases of AD (9 males and 13 females; ages 57–93 yr, average 78 yr) using NIA and CERAD criteria

From the Institute of Pathology (AN, GP, GA, KH, AT, EKB, CSA, RPB, MAS) and Department of Epidemiology and Biostatistics (PKJ), Case Western Reserve University, Cleveland, Ohio; Department of Psychiatry and Neurology (AN, SC), Asahikawa Medical College, Asahikawa, Japan; Cuyahoga County Coroner's Office (EKB), Cleveland, Ohio; Panacea Pharmaceuticals, Rockville, Maryland (HG); Pharmaceutical Research Laboratories I, Pharmaceutical Research Division (KH), Takeda Chemical Industries Ltd., Osaka, Japan; and Department of Neurology (TW, SS), Graduate School of Medicine, Kyoto University, Kyoto, Japan.

Correspondence to: Mark A. Smith, PhD, Institute of Pathology, Case Western Reserve University, 2085 Adelbert Road, Cleveland, Ohio 44106.

This work was supported by the National Institutes of Health (AG09287 and AG14249), Alzheimer's Association (Stephanie B. Overstreet Scholars [IIRG-00-2163], TLL-99-1872, and ZEN-99-1789), and the Japan Society for the Promotion of Science (Grant-in-Aid for Scientific Research (c) 12670918).

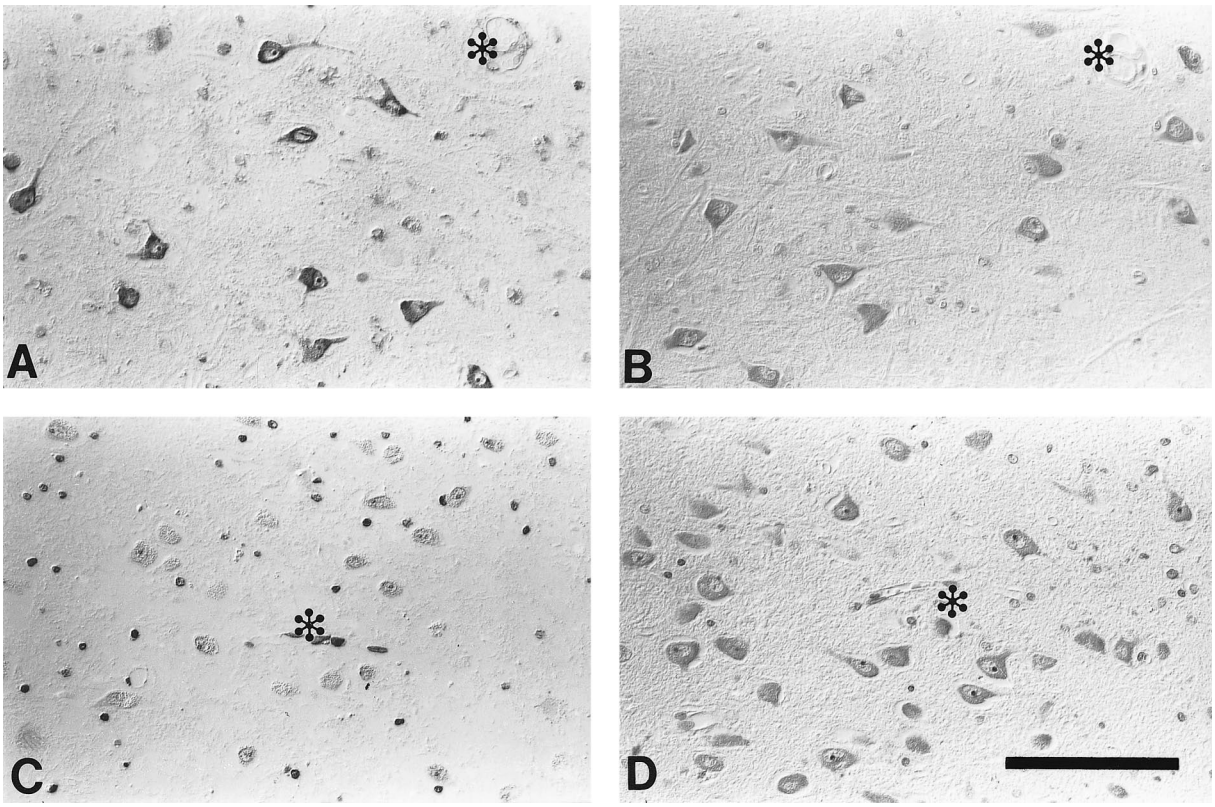

Fig. 1. Among cases of AD, hippocampal pyramidal neurons show considerable individual variation in 8OHG immunoreactivity with 1F7 antibody (A, C) in spite of similar staining levels of cellular RNA with methyl green-pyronin method (B, D). A 79-yr-old case (A, B) and an 83-yr-old case (C, D) of AD. Note the relative uniformity of staining among neurons within the same case. *Indicates landmark blood vessel in adjacent section. Differential interference contrast. Scale bar = 100 μm.

(22, 23), as well as from a consecutive series of 17 controls without dementia (12 males and 5 females; ages 62–86 yr, average 74 yr). The cases of AD were not preselected based on any feature analyzed in this study. Postmortem intervals prior to fixation were 2 to 23 hours (h). Duration of dementia (3–16 yr, average 8.2 yr) was known from clinical records in 16 AD cases. The ApoE genotype of the AD cases was determined for all 22 AD cases by standard procedures (24) and found to be ϵ4/ ϵ4 (n = 3); ϵ3/ ϵ4 (n = 11); ϵ3/ ϵ3 (n = 5); ϵ2/ ϵ4 (n = 1); ϵ2/ ϵ3 (n = 2). The ApoE ϵ4 allele frequency was 0.41, which is consistent with the results from a study of 679 subjects with AD (ϵ4 allele frequency = 0.46) (25). Hippocampal slices (~1-cm thick and including the surrounding subiculum, entorhinal cortex, and adjacent temporal neocortex) were fixed in methacarn (methanol: chloroform: acetic acid, 6:3:1) for 16 h at 4°C, dehydrated through graded ethanol followed by xylene, and embedded in paraffin. Six-μm-thick sections were cut and mounted on Silane® (Sigma)-coated glass slides.

Immunocytochemistry and Antibodies

Following deparaffinization with xylene, sections were hydrated through graded ethanol. Endogenous peroxidase activity in the tissue was eliminated by a 30-minute (min) incubation with 3% H_2O_2 in methanol and nonspecific binding sites were blocked in a 30-min incubation with 10% normal goat serum (NGS) in Tris-buffered saline (150 mM Tris-HCl, 150 mM NaCl, pH 7.6). To detect oxidized nucleosides, we used a mouse monoclonal antibody against 8OHG, 1F7 (26) (1:30; gift of Regina M. Santella, Division of Environmental Sciences, School of Public Health, Columbia University, New York) after treatment with 10 μg/ml proteinase K (Boehringer Mannheim, Indianapolis, IN) in PBS (pH = 7.4) for 40 min at 37°C. Immunostaining was developed by the peroxidase-antiperoxidase procedure (27) by using 0.75 mg/ml 3,3′-diaminobenzidine cosubstrate in 0.015% H_2O_2, 50 mM Tris-HCl, pH 7.6 for exactly 10 min. Although 1F7 recognizes RNA-derived 8OHG as well as DNA-derived 8OHdG with similar binding affinities (26), we have confirmed that 1F7 immunolabeling in neurons in AD is predominantly in RNA by the pretreatment with DNase or RNase (10) as well as by immunoelectronmicroscopy, which showed that most 8OHG is present in the endoplasmic reticulum. Additionally, protein oxidation was studied in 7 cases of AD, assessing the level of nitrotyrosine with a monoclonal antibody, 7A2 (5) (1:100; gift of Joseph S. Beckman, Department of Anesthesiology, University of Alabama, Birmingham, AL). Nitrotyrosine was used as a marker since nitration is not directly related to protein crosslinking and alterations that make protein resistant to turnover. Furthermore, while nitrotyrosine was initially thought to be specifically derived from peroxynitrite attack of tyrosines, more recent studies suggest that in AD, nitrotyrosine is also generated by peroxidative nitration (Cash, Perry, and Smith, unpublished observations). To estimate comparative levels of cellular RNA, we performed the methyl green-pyronin method (28) that differentially stains DNA and

RNA. We confirmed the specificity for RNA by showing that RNase treatment [RNase A (Sigma), 1 mg/ml for 16 h] removes methyl green-pyronin positive staining for RNA. Only nuclei remain stained blue, indicating DNA resistant RNase. Conversely, treating with DNAse I and S1 nuclease (Boehringer Mannheim; 10U/μl of each for 16 h) removes all nuclear staining, leaving red cytoplasmic and faint nuclear staining, indicating RNA resistant to DNase. We carefully controlled the pH (4.8) of the staining solution, the staining period (45 min), and steps of the final dehydration (4 dips in 95% ethanol followed by 4 dips in absolute ethanol). Reproducibility of the staining method was confirmed by the indistinguishable findings made when adjacent serial sections were stained.

Aβ deposits of senile plaque were immunostained with a mouse monoclonal antibody, 4G8 (1:1,000, Senetek, St. Louis, MO), specific for Aβ 17–24 amino acids. Neurofibrillary tangles (NFT) were identified by immunostaining with a mouse monoclonal antibody to phosphorylated τ, AT8 (1:500, Biosource International, Camarillo, CA) or rabbit antiserum to τ (29) (1:1,000), as well as by counterstaining the sections with Congo red and viewing under plane polarized light. Additionally, sections of 3 AD cases were double immunostained with 1F7 and the antiserum to τ, by using the alkaline phosphatase-antialkaline phosphatase method with fast blue BB-naphthol AS-MX and the peroxidase-antiperoxidase method with diaminobenzidine, respectively.

Brain ultrastructural localization of 8OHG with IF7 was performed in a 67-yr-old AD patient who was not part of the series, and with a postmortem interval of 1.5 h. The tissue was fixed in 2% paraformaldehyde, 0.5% glutaraldehyde, 0.5 mM calcium chloride, 0.1 M sodium cacodylate (pH 7.4). Vibratome sections (60 μm) were treated with 10 μg/ml proteinase K (Boehringer Mannheim) in PBS (pH 7.4) for 40 min at 37°C prior to application of IF7. Immunoreaction was detected with goat antiserum to mouse Ig conjugated to collodial gold (17 nm) (30). Following immunoreaction, the tissue was fixed in 2.5% glutaraldehyde and postfixed in 1.0% OsO_4. The specimens were dehydrated and embedded in Spurr's medium, sectioned at 60–100 nm, contrasted with lead and uranyl salts, and examined in a JEOL100CX electron microscope at 80 kV.

Relative Scale of 8OHG and Aβ Deposition

All measurements were performed in stratum pyramidale of prosubiculum adjacent to the CA1 field of hippocampus using a Quantimet 570C Image Processing and Analysis System (Leica) linked to a COHU Solid State Camera mounted on a Leitz Laborlux 12 ME ST microscope.

The intensity of immunoreaction with 1F7 was evaluated by measuring the average optical density (OD) in an area comprising the cytoplasm and nucleus, as we described previously (10). Three adjacent fields (each field = 460 μm × 428 μm) were selected, and in each field of the video camera, 5 pyramidal neurons sectioned near their equator (based on a section plane that included the nucleolus) were selected and outlined manually so that the ratio of the area of the nucleus to cytoplasm was rather constant. The nucleus was included because damage to RNA was nuclear as well as cytoplasmic. The average OD measurement was obtained for each of the 3 fields and averaged. Finally, the OD value was corrected for background by subtracting the OD of the white matter on the same section.

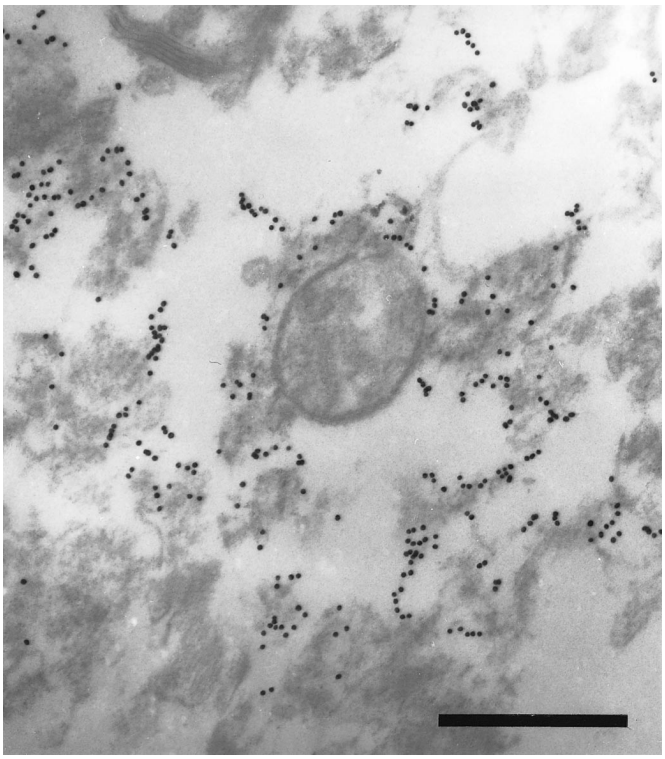

Fig. 2. Electron micrograph showing 8OHG immunolabeling for a case of AD. The majority of colloidal gold is associated with ribosomal structures, which is consistent with our previous finding that cytoplasmic RNA species, possibly ribosomal RNA, transfer RNA, and/or messenger RNA, are major target of nucleic acid oxidation in vulnerable neurons (10). Indirect immunogold. Scale bar = 1 μm.

For the measurement of the extent of Aβ deposition, 3 adjacent fields were selected to include the same area used to measure 1F7 immunoreactivity in an adjacent serial section. The area of Aβ deposits immunostained with 4G8 was determined with gray scale thresholding according to the methods used by Hyman et al (31). The sum of the areas of Aβ deposits was divided by the total area to give the percentage of Aβ burden.

All measurements were done under the same optical and light conditions, as well as using an electronic shading correction to compensate for any unevenness that might be present in the illumination. Statistical analysis was performed with ANOVA or Mann-Whitney *U*-test, as well as log-linear regression analysis, Spearman's rank correlation, and Kendall's rank correlation, using StatView 4.11 program (Abacus Concepts, Berkeley, CA).

RESULTS

In cases of AD, 8OHG immunoreactivity was prominent in the neuronal cytoplasm in the hippocampus, subiculum, and entorhinal cortex, as well as temporal neocortex (Figs. 1A, 3A). Ultrastructural examination

TABLE 1
Comparison of Neuronal Immunoreactivity between 8OHG and Nitrotyrosine in AD

Age	PMI (h)	8OHG (1 F7)	Nitrotyrosine (7 A2)	Amyloid β burden (%)*
57 y	2	+++	++	2.7%
60 y	9	++	+	3.0%
76 y	4	++	+	2.3%
83 y	4	+	+	2.9%
84 y	5	+	+	5.7%
74 y	9	±	±	5.4%
78 y	9	±	±	7.0%

+++, very strongly positive; ++, strongly positive; +, positive; ±, faintly positive.

* The area of amyloid β (%) was evaluated in the hippocampal prosubiculum in immunostained sections (4G8).

PMI, postmortem interval.

showed that the majority of 8OHG immunoreactivity was associated with ribosomes in the endoplasmic reticulum; most mitochondria showed no detectable 8OHG (Fig. 2). Among the cases of AD, there was considerable individual variation of the immunointensity of 8OHG (Fig. 1A, C). This variation could not be explained by differences in levels of RNA, since sections stained with the methyl green-pyronine method showed similar intensity among all the AD cases (Fig. 1B, D). We also found variation in the immunointensity of nitrotyrosine with a concordance to changes in 8OHG. That protein and nucleic acid immunointensities coincided suggests that the variation of either reflects global levels of oxidative damage (Table 1).

When we investigated relative levels of immunointensities, we observed that AD cases with abundant Aβ plaques showed the least intense immunostaining of neuronal 8OHG (Fig. 3). The same relationship was noted between the protein oxidation marker, nitrotyrosine immunoreactivity, and percentage of Aβ burden (Table 1). Relative scale measurements for immunointensity of neuronal 8OHG and area of Aβ burden (%) revealed a significant inverse relationship between the levels of neuronal 8OHG and the extent of Aβ burden in AD ($p = 0.0001$) (Fig. 4A). Among our AD cases, we found a positive relationship between the percentage of Aβ burden and duration of dementia ($p < 0.01$) (Fig. 4C), and therefore, it is not surprising that neuronal 8OHG levels were also inversely related to disease duration ($p < 0.03$) (Fig. 4B).

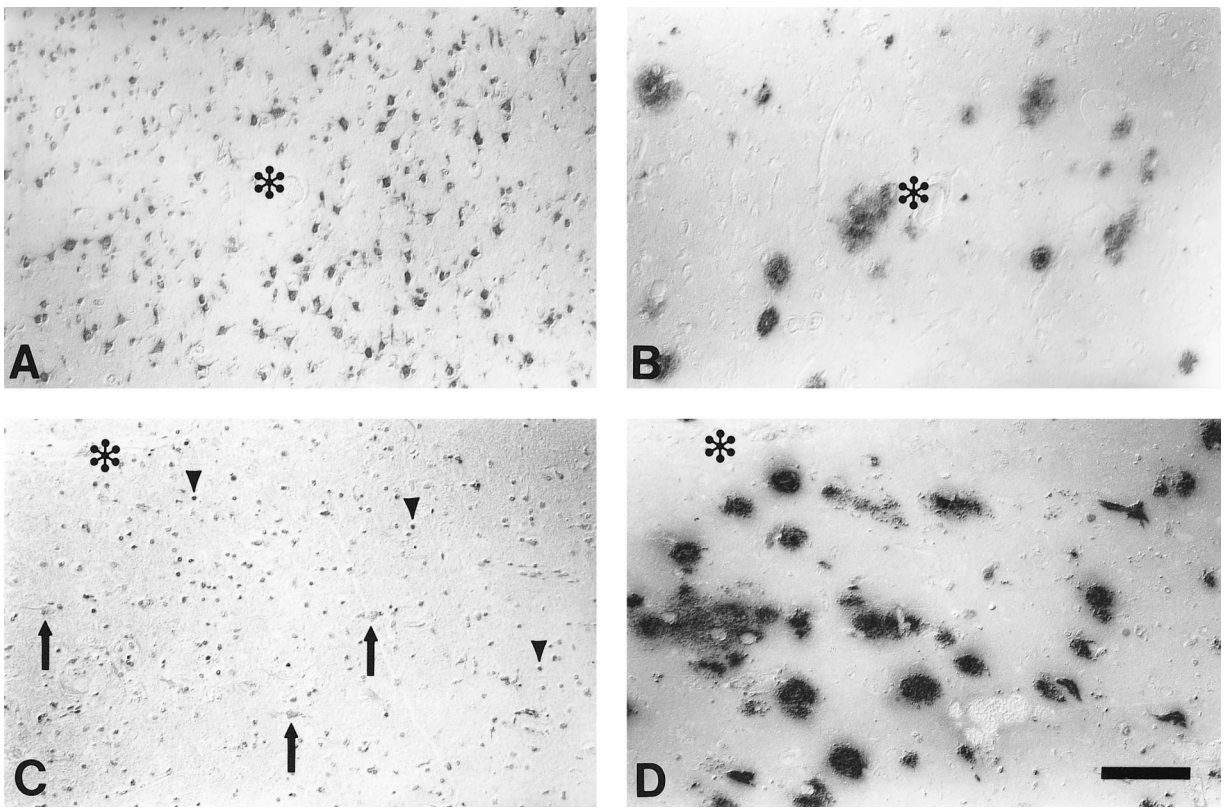

Fig. 3. Aβ deposition is associated with decreased levels of neuronal 8OHG immunoreactivity in AD. Entorhinal cortex of a 76-yr-old AD case shows prominent 8OHG immunoreactivity with 1F7 antibody (A) with limited Aβ deposition (4G8) (B). In contrast, neuronal 8OHG immunoreactivity (arrows) in entorhinal cortex of an 84-yr-old AD case with abundant Aβ deposition is less intense (C, D). Note that in this case, glial nuclei (arrowheads) show positive 8OHG immunoreaction (C). *Indicates landmark blood vessel in adjacent section. Differential interference contrast. Scale bar = 100 μm.

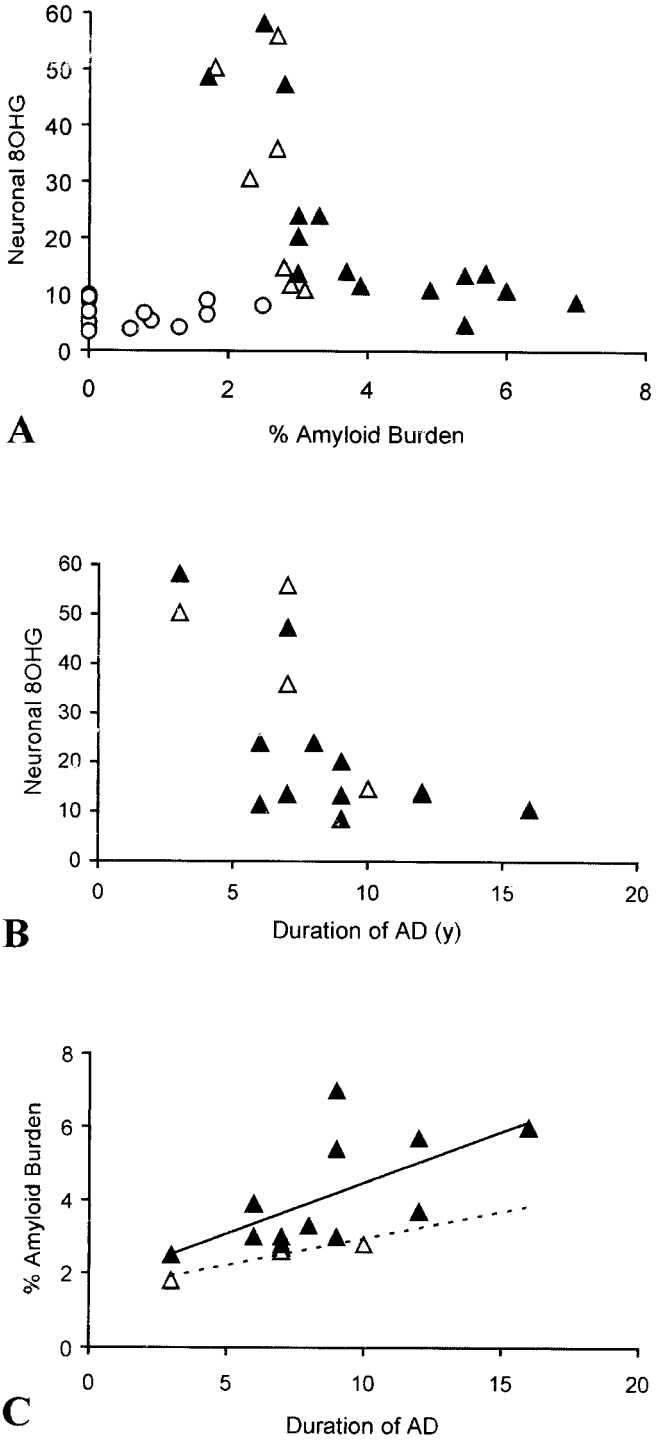

Fig. 4. Relation of neuronal 8OHG, levels of Aβ deposition and disease duration in cases of AD, with ApoE4 (▲) or without ApoE4 (△), and in controls (○). A: Relative scale measurements of neuronal 8OHG immunoreactivity and area of Aβ burden (%) in the prosubiculum of 22 AD cases and 17 age-matched controls. Levels of neuronal 8OHG decrease exponentially with increasing Aβ burden in AD, while in controls no significant association is noted between them. In AD cases, Spearman's rank correlation coefficient (r_s) is −0.84 (p = 0.0001). This inverse relationship among cases of AD is statistically significant in the ApoE4-positive group (▲) (n = 15, r_s = −0.86, p < 0.002) but only equivocal level in the ApoE4-negative group (△) (n = 7, p = 0.05). B: Similar pattern of exponential decrease in neuronal 8OHG is noted by increasing disease duration (r_s = −0.59, p < 0.03). C: In those cases, the percentage of Aβ burden increases as a function of the disease duration in a linear fashion (r = 0.66, p < 0.01). This linear relationship is statistically significant in ApoE4-positive cases (▲) (n = 7, r = 0.64, p < 0.03) but not in ApoE4-negative cases (△) (n = 4, p > 0.08).

When the AD cases were divided into ApoE ϵ4-positive and ApoE ϵ4-negative groups, we noted that those cases carrying ApoE ϵ4 showed a significant correlation between neuronal 8OHG and percentage of Aβ burden, while those lacking ApoE ϵ4 showed only an equivocal level of statistical significance, as summarized in Table 2. No direct effect of ApoE ϵ4 was detected on the levels of 8OHG since there were no significant differences in the 8OHG levels between ApoE ϵ4-positive and ϵ4-negative groups (p > 0.2 by Mann-Whitney *U*-test), as well as among 3 different groups of ApoE genotype, ϵ4/ϵ4, ϵ3/ϵ4 and ϵ3/ϵ3 (p > 0.5 by ANOVA). Aβ burden increases in a linear fashion as a function of the disease duration. This correlation was statistically significant among all AD cases (p < 0.01), among those carrying ApoE ϵ4 (p < 0.03; the reduced significance of ApoE ϵ4 cases compared to all AD cases, n = 22 versus n = 15, is due to reduced number of cases), but not in those lacking ApoE ϵ4 (p > 0.05) (Fig. 4C), suggesting that the relationship of increased Aβ with disease duration is ApoE ϵ4-dependent. This heterogeneity in the amount of Aβ with duration in ApoE ϵ4-positive versus ApoE ϵ4-negative groups may explain in part why there has been controversy about whether Aβ burden increases with the progression of AD. However, we found significantly higher percentage of Aβ burden (p < 0.03 by Mann-Whitney *U*-test) in ApoE ϵ4-positive cases (average, 4.1% [ϵ4-homozygotes, 4.0%; ϵ4-heterozygotes, 4.1%]) than ApoE ϵ4-negative cases (2.6%), as shown in previous studies (32, 33). The extent to which Aβ deposition is increased with disease duration is more significant in cases carrying ApoE ϵ4 than in those lacking ApoE ϵ4.

When we investigated the sections immunostained with the antibody to 8OHG and counterstained with Congo red, we observed that neurons containing NFT showed reduced 8OHG immunoreactivity. Double immunostaining with the antibodies to 8OHG and τ revealed little overlap between 8OHG and τ immunoreactivity as well as low levels of 8OHG immunoreactivity in the cytoplasm surrounding NFT (Fig. 5). We found a significant decrease of 8OHG in NFT-positive neurons independent of the amount of Aβ burden and ApoE genotype (Table 3).

TABLE 2
Correlation between Neuronal 8OHG and Amyloid β Burden (%) and between Neuronal 8OHG and Disease Duration by 3 Different Statistical Analyses

	Log-linear regression analysis†	Spearman's rank correlation	Kendall's rank correlation
8OHG and Aβ burden (%)			
All AD (n = 22)	−0.77****	−0.84****	−0.66****
AD, ApoE4 (+) (n = 15)	−0.82***	−0.86**	−0.72***
AD, ApoE4 (−) (n = 7)	−0.67 (n.s.)	−0.79 (n.s.)	−0.68*
Control (n = 17)	n.a.	−0.07 (n.s.)	−0.04 (n.s.)
8OHG and Duration			
All AD (n = 16)	−0.70**	−0.59*	−0.49**
AD, ApoE4 (+) (n = 12)	−0.68*	−0.50 (n.s.)	−0.40 (n.s.)
AD, ApoE4 (−) (n = 4)	−0.66 (n.s.)	−0.63 (n.s.)	−0.55 (n.s.)

Values shown are correlation coefficients.
† log (neuronal 8OHG) versus log (percentage of amyloid β burden) or log (neuronal 8OHG) versus log (duration). Asterisks indicate statistically significant p-value, as **** $p \leq 0.0001$, *** $p < 0.001$, ** $p < 0.01$, and * $p < 0.05$. n.a. = not available (11 controls showed no amyloid β burden). n.s. = not significant.

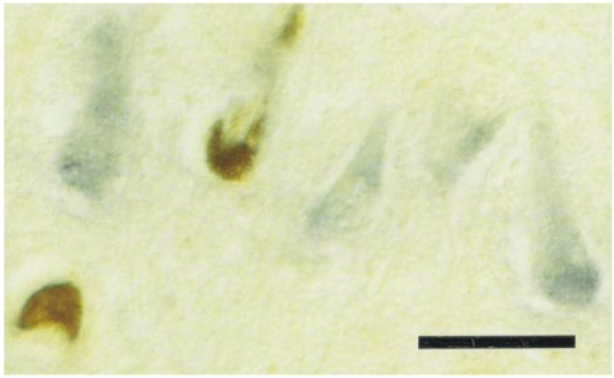

Fig. 5. Double immunolabeling with 1F7 antibody and antiserum against τ shows no overlap between 8OHG (blue) and τ (brown) in neurons in the stratum pyramidal of the hippocampus from a 60-yr-old AD case. Differential interference contrast. Scale bar = 25 μm.

TABLE 3
Effect of the Presence of Neurofibrillary Tangles (NFT) on the Relative 8OHG in Neurons in AD

Age	Relative 8OHG: NFT(−) neuron	Relative 8OHG: NFT (+) neuron	Relative 8OHG: Decrease (%)	p**	ApoE geno-type	Aβ burden (%)
57 y	71.5 (5.5)*	38.9 (3.1)	45.6%	<0.01	3/3	2.7%
74 y	55.6 (6.2)	24.3 (3.2)	56.3%	<0.01	3/3	2.7%
93 y	16.1 (1.5)	9.6 (0.8)	40.4%	<0.01	3/3	2.8%

Three AD cases with similar amount of Aβ burden and with ApoE ε3/3 genotype were selected to test the effect of NFT on the relative 8OHG levels independently of the effects of Aβ burden and ApoE genotype. In the stratum pyramidal of the hippocampus, 8OHG immunoreactivity with 1F7 antibody was measured in 5 pairs of adjacent NFT-positive and NFT-negative neurons showing nucleolus that were selected in sections counterstained with Congo red under plane polarized light.
* Values are expressed in mean (SE).
** p-values are evaluated within each case by Mann-Whitney *U* test.

Levels of 8OHG immunoreactivity were not related to the agonal state of the AD cases before death or to postmortem intervals (10). Among AD cases, there was no difference in 8OHG related to cause of death, i.e. acute cardiac failure (myocardial infarction or cardiac arrhythmia; n = 3), chronic heart or lung disease (congestive cardiac failure, chronic obstructive pulmonary disease, or lung fibrosis; n = 6), respiratory or urinary tract infection (n = 4), and emaciation (n = 3) ($p > 0.5$ by ANOVA). In addition, no gender difference was found in either AD ($p > 0.9$ by Mann-Whitney *U*-test) or control ($p > 0.3$) cases.

DISCUSSION

In this study of AD, we found an inverse relationship between levels of oxidative damage to both Aβ deposits and duration of dementia. Further, formation of intraneuronal NFT was also associated with reduced oxidative damage. Our findings demonstrated not only that onset of oxidative damage is an early event in AD, but also that the level of oxidative damage observed in neurons decreases in association with the abundance of histopathology. We found similar results with Down syndrome cases, where AD neuropathology predictably forms in early life (21), as well as in cases of familial AD (34).

Our observations could be explained if RNA is depleted in neurons with severe pathological changes (35, 36), however, microdensitometry showed that RNA depletion in AD is unrelated to the presence of NFT (36). In this study, the level of 8OHG immunoreactivity was independent of the level of RNA, which was estimated by the staining intensity of the methyl green-pyronin method (Fig. 1). Furthermore, NFT actually accumulate RNA (37), suggesting that decreased 8OHG levels in

NFT-bearing neurons reflects a bona fide decrease in damage from reactive oxygen.

Neuronal RNA oxidation increase has not only been detected in the cerebral cortex of AD (10), but also in the substantia nigra of Parkinson disease (38). The consequence of oxidized RNA is not fully understood; however, it has been suggested that oxidatively damaged nucleic acids may interfere with correct base pairing and could compromise the accuracy of transcription and translation (39). In this regard, it is interesting to note the recent evidence showing protein sequence abnormalities in vulnerable neurons of AD (40).

Possible Sources of Reactive Oxygen in AD

Our findings suggest that the changes related to increased peroxidative damage in AD are upstream pathological events that are primarily restricted to the neuronal cytoplasm. Because 8OHG is produced by the attack of hydroxyl radicals that can diffuse only nanometer distances, hydroxyl radicals must be generated in the cytosol in intimate proximity to RNA. While we do not know the source of the hydroxyl radicals, mitochondrial dysfunction (41), intraneuronal Aβ accumulation (42), and redox-active metals (43) are candidates, and it is tempting to consider that redox active metals bound in close proximity to RNA are involved.

Mitochondria produce superoxide radical as part of normal respiration and in greater quantities when respiration is compromised. While the superoxide radical diffuses poorly past membranes, its dismutation product, hydrogen peroxide, can diffuse freely. More importantly, in the presence of redox-active metals (e.g. iron or copper), hydrogen peroxide is the biological substrate for hydroxyl radical generation. Therefore, mitochondrial abnormalities may promote oxidative damage not only by supplying excess hydrogen peroxide, but also through lysosomal degradation of damaged mitochondria and consequent release of heme iron into the cytosol (44).

Another candidate source of ROS in AD is redox metals bound to Aβ, which can generate hydrogen peroxide directly (45, 46). That intraneuronal Aβ accumulation is prominent at an early stage of AD, and becomes less noticeable with disease progression (42), parallels the decline of oxidative damage with abundant AD pathology or longer duration of AD shown in this study. While enrichment of redox-active metals in the senile plaques and NFT (43) supports the AD pathology as a possible source of ROS, our observations of no damage surrounding Aβ deposits and reduction near NFT in this study strongly contradict this possibility. Whether lesion-associated metals display pro-oxidant or antioxidant activity would depend on the balance among cellular reductants and oxidants in the local microenvironment (43). In this regard, we recently found that zinc, a redox-inert antioxidant as well as a strong mediator of Aβ assembly, showed an inhibitory role in hydrogen peroxide-mediated Aβ toxicity. The deposition of Aβ may represent the redox silencing and entombment of Aβ by zinc (47, 48).

Antioxidant Defenses in AD Brain

The activities and expression of a number of antioxidant enzymes such as Cu/Zn- and Mn-superoxide dismutase, glutathione peroxidase, glutathione reductase, and catalase have been studied in AD and could be in part responsible for the decrease in oxidative damage we observed. While generalized levels of Cu/Zn- and Mn-superoxide dismutase are not consistently changed in AD (1), immunocytochemical studies revealed focal increases in Cu/Zn-superoxide dismutase and catalase with exact localization to NFT and senile plaques (49), as well as coexpression of Mn-superoxide dismutase and τ in pyramidal neurons (50). Furthermore, the antioxidant enzyme, hemeoxygenese-1, is localized to NFT (51, 52). Upregulation of these antioxidant enzymes may be the mechanistic basis for the decreased RNA and protein oxidation in neurons with NFT.

ApoE and Oxidative Stress

In sporadic and late-onset familial AD, ApoE ϵ4 allele is the major genetic risk factor that lowers the average age of onset, decreases neuronal metabolism, and increases Aβ burden (32, 33, 53, 54). Decreased glucose metabolism related to the ApoE ϵ4 allele was observed in AD subjects 2 decades before the median age of onset (55). Moreover, the isoforms of ApoE have metal binding and antioxidant activity with E2 > E3 > E4 (56). In this study, no direct allele-specific effect of ApoE on the levels of steady-state markers of oxidative damage was found, in contrast to the studies showing the significant association between cumulative damage of lipid peroxidation products and ApoE ϵ4 allele (7, 13, 14) (The sample size of AD subjects is similar to our study [n = 22] compared to these prior studies, i.e. n = 13, 28, and 21 in references 7, 13, and 14, respectively). This discrepancy may suggest a very early, or even preclinical, involvement of ApoE ϵ4 in the oxidative stress in AD. This, in turn, triggers either compensatory mechanisms against oxidative stress or further reduction in metabolic activity in advanced stages of AD that results in lower reactive oxygen production late in the disease. Interestingly, we found that an increased abundance of Aβ deposits, as well as the strong inverse correlation between Aβ deposits and oxidative stress, were associated with the ApoE ϵ4 allele.

REFERENCES

1. Markesbery WR, Carney JM. Oxidative alterations in Alzheimer's disease. Brain Pathol 1999;9:133–46
2. Smith MA, Rottkamp CA, Nunomura A, Raina AK, Perry G. Oxidative stress in Alzheimer's disease. Biochem Biophys Acta 2000; 1502:139–44

3. Smith CD, Carney JM, Starke-Reed PE, et al. Excess brain protein oxidation and enzyme dysfunction in normal aging and Alzheimer disease. Proc Natl Acad Sci USA 1991;88:10540–43
4. Smith MA, Perry G, Richey PL, et al. Oxidative damage in Alzheimer's. Nature 1996;382:120–21
5. Smith MA, Harris PLR, Sayre LM, Beckman JS, Perry G. Widespread peroxynitrite-mediated damage in Alzheimer's disease. J Neurosci 1997;17:2653–57
6. Sayre LM, Zelasko DA, Harris PLR, Perry G, Salomon RG, Smith MA. 4-Hydroxynonenal-derived advanced lipid peroxidation end products are increased in Alzheimer's disease. J Neurochem 1997; 68:2092–97
7. Montine KS, Recch E, Neely MD, et al. Distribution of reducible 4-hydroxynonenal adduct immunoreactivity in Alzheimer disease is associated with APOE genotype. J Neuropathol Exp Neurol 1998; 57:415–25
8. Mecocci P, MacGarvey U, Beal MF. Oxidative damage to mitochondrial DNA is increased in Alzheimer's disease. Ann Neurol 1994;36:747–51
9. Gabbita SP, Lovell MA, Markesbery WR. Increased nuclear DNA oxidation in the brain in Alzheimer's disease. J Neurochem 1998; 71:2034–40
10. Nunomura A, Perry G, Pappolla MA, et al. RNA oxidation is a prominent feature of vulnerable neurons in Alzheimer's disease. J Neurosci 1999;19:1959–64
11. Strittmatter WJ, Weisgraber KH, Huang DY, et al. Binding of human apolipoprotein E to synthetic amyloid β peptide: Isoform-specific effects and implications for late-onset Alzheimer disease. Proc Natl Acad Sci USA 1993;90:8098–102
12. Smith JD, Sikes J, Perry G, Smith MA. ApoE: Isoform specific antioxidant activity [abstract]. Neurobiol Aging 1998;19:S222
13. Ramassamy C, Averill D, Beffert U, et al. Oxidative damage and protection by antioxidants in frontal cortex of Alzheimer's disease is related to the apolipoprotein E genotype. Free Radic Biol Med 1999;27:544–53
14. Tamaoka A, Miyatake F, Matsuno S, et al. Apolipoprotein E allele-dependent antioxidant activity in brains with Alzheimer's disease. Neurology 2000;54:2319–21
15. Behl C, Davis JB, Lesley R, Schubert D. Hydrogen peroxide mediates amyloid β protein toxicity. Cell 1994;77:817–27
16. Hensley K, Carney JM, Mattson MP, et al. A model for β-amyloid aggregation and neurotoxicity based on free radical generation by the peptide: Relevance to Alzheimer disease. Proc Natl Acad Sci USA 1994;91:3270–74
17. Yan SD, Yan SF, Chen X, et al. Non-enzymatically glycated tau in Alzheimer's disease induces neuronal oxidant stress resulting in cytokine gene expression and release of amyloid β-peptide. Nature Med 1995;1:693–99
18. Frederikse PH, Garland D, Zigler JS Jr, Piatigorsky J. Oxidative stress increases production of β-amyloid precursor protein and β-amyloid (Aβ) in mammalian lenses, and Aβ has toxic effects on lens epithelial cells. J Biol Chem 1996;271:10169–74
19. Misonou H, Morishima-Kawashima M, Ihara Y. Oxidative stress induces intracellular accumulation of amyloid β-protein (Aβ) in human neuroblastoma cells. Biochemistry 2000;39:6951–59
20. Sayre LM, Perry G, Smith MA. In situ methods for detection and localization of oxidative stress: Application in neurodegenerative disorders. In: Wetzel R, ed. Methods of enzymology, Vol. 309. San Diego: Academic Press, 1999:133–52
21. Nunomura A, Perry G, Pappolla MA, et al. Neuronal oxidative stress precedes amyloid-β deposition in Down syndrome. J Neuropathol Exp Neurol 2000;59:1011–17
22. Khachaturian ZS. Diagnosis of Alzheimer's disease. Arch Neurol 1985;42:1097–105
23. Mirra SS, Heyman A, McKeel D, et al. The Consortium to Establish a Registry for Alzheimer's Disease (CERAD). Part II. Standardization of the neuropathologic assessment of Alzheimer's disease. Neurology 1991;41:479–86
24. Hixson JE, Vernier DT. Restriction isotyping of human apolipoprotein E by gene amplification and cleavage with *Hha*I. Lipid Res 1990;31:545–48
25. Blacker D, Haines JL, Rodes L, et al. ApoE-4 and age at onset of Alzheimer's disease: The NIMH genetics initiative. Neurology 1997;48:139–47
26. Yin B, Whyatt RM, Perera FP, Randall MC, Cooper TB, Santella RM. Determination of 8-hydroxydeoxyguanosine by an immunoaffinity chromatography-monoclonal antibody-based ELISA. Free Radic Biol Med 1995;18:1023–32
27. Sternberger LA. Immunocytochemistry. Third edition, New York: Wiley, 1986
28. Bancroft JD, Stevens A. Theory and practice of histological techniques. Fourth edition, New York: Churchill Livingstone, 1996
29. Perry G, Kawai M, Tabaton M, et al. Neuropil threads of Alzheimer's disease show a marked alteration of the normal cytoskeleton. J Neurosci 1991;11:1748–55
30. Perry G, Rizzuto N, Autilio-Gambetti L, Gambetti P. Paired helical filaments from Alzheimer disease patients contain cytoskeletal components. Proc Natl Acad Sci USA 1985;82:3916–20
31. Hyman BT, Marzloff K, Arriagada PV. The lack of accumulation of senile plaques or amyloid burden in Alzheimer's disease suggests a dynamic balance between amyloid deposition and resolution. J Neuropathol Exp Neurol 1993;52:594–600
32. Gomez-Isla T, West HL, Rebeck GW, et al. Clinical and pathological correlates of apolipoprotein E ϵ4 in Alzheimer's disease. Ann Neurol 1996;39:62–70
33. McNamara MJ, Gomez-Isla T, Hyman BT. Apolipoprotein E genotype and deposits of Aβ40 and Aβ42 in Alzheimer disease. Arch Neurol 1998;55:1001–4
34. Nunomura A, Chiba S, Lippa CF, Smith MA, Perry G. Increasing amyloid ß 42 deposition is associated with decreasing neuronal RNA oxidation in Down's syndrome and familial Alzheimer's disease [abstract]. Brain Pathol 2000;10:783
35. Mann DMA, Neary D, Yates PO, Lincoln J, Snowden JS, Stanworth P. Alterations in protein synthetic capability of nerve cells in Alzheimer's disease. J Neurol Neurosurg Psychiatry 1981;44:97–102
36. Doebler JA, Markesbery WR, Anthony A, Rhoads RE. Neuronal RNA in relation to neuronal loss and neurofibrillary pathology in the hippocampus in Alzheimer's disease. J Neuropathol Exp Neurol 1987;46:28–39
37. Ginsberg SD, Crino PB, Lee VM-Y, Eberwine JH, Trojanowski JQ. Sequestration of RNA in Alzheimer's disease neurofibrillary tangles and senile plaques. Ann Neurol 1997;41:200–209
38. Zhang J, Perry G, Smith MA, et al. Parkinson's disease is associated with oxidative damage to cytoplasmic DNA and RNA in substantia nigra neurons. Am J Pathol 1999;154:1423–29
39. Rhee Y, Valentine MR, Termini J. Oxidative base damage in RNA detected by reverse transcriptase. Nucleic Acids Res 1995;23: 3275–82
40. van Leeuwen FW, de Kleijn DPV, van den Hurk HH, et al. Frameshift mutants of β amyloid precursor protein and ubiquitin-B in Alzheimer's and Down patients. Science 1998;279:242–47
41. Hirai K, Aliev G, Nunomura A, et al. Mitochondrial abnormalities in Alzheimer disease. J Neurosci 2001;21:3017–23
42. Gouras GK, Tsai J, Naslund J, et al. Intraneuronal Aβ42 accumulation in human brain. Am J Pathol 2000;156:15–20
43. Sayre LM, Perry G, Harris PLR, Liu Y, Schubert KA, Smith MA. In situ oxidative catalysis by neurofibrillary tangles and senile plaques in Alzheimer disease: A central role for bound transition metals. J Neurochem 2000;74:270–79

44. Perry G, Nunomura A, Hirai K, Takeda A, Aliev G, Smith MA. Oxidative damage in Alzheimer's disease: The metabolic dimension. Int J Dev Neurosci 2000;18:417–21
45. Huang X, Cuajungco MP, Atwood CS, et al. Cu (II) potentiation of Alzheimer Aβ neurotoxicity. Correlation with cell-free hydrogen peroxide production and metal reduction. J Biol Chem 1999;274: 37111–16
46. Rottkamp CA, Raina AK, Zhu X, et al. Redox-active iron mediates amyloid-β toxicity. Free Radic Biol Med 2001;30:447–50
47. Cuajungco MP, Goldstein LE, Nunomura A, et al. Evidence that the β-amyloid plaques of Alzheimer's disease represent the redox-silencing and entombment of Aβ by zinc. J Biol Chem 2000;275: 19439–42
48. Moreira P, Pereira C, Santos MS, Oliveira C. Effect of zinc ions on the cytotoxicity induced by the amyloid β-peptide. Antiox Redox Signal 2000;2:317–25
49. Pappolla MA, Omar RA, Kim KS, Robakis NK. Immunohistochemical evidence of oxidative stress in Alzheimer's disease. Am J Pathol 1992;140:621–28
50. Furuta A, Price DL, Pardo CA, et al. Localization of superoxide dismutases in Alzheimer's disease and Down's syndrome neocortex and hippocampus. Am J Pathol 1995;146:357–67
51. Smith MA, Kutty RK, Richey PL, et al. Heme oxygenase-1 is associated with the neurofibrillary pathology of Alzheimer's disease. Am J Pathol 1994;145:42–47
52. Takeda A, Smith MA, Avila J, et al. In Alzheimer disease, heme oxygenase is coincident with Alz50, an epitope of τ induced by 4-hydroxy-2-nonenal modification. J Neurochem 2000;75:1234–41
53. Roses AD. Apolipoprotein E affects the rate of Alzheimer disease expression: β-amyloid burden is a secondary consequence dependent on APOE genotype and duration of disease. J Neuropathol Exp Neurol 1994;53:429–37
54. Salehi A, Dubelaar EJG, Mulder M, Swaab DF. Aggravated decrease in the activity of nucleus basalis neurons in Alzheimer's disease is apolipoprotein E-type dependent. Proc Natl Acad Sci USA 1998;95:11445–44
55. Reiman EM, Caselli RJ, Yun LS, et al. Preclinical evidence of Alzheimer's disease persons homozygous for the ϵ4 allele for apolipoprotein E. N Engl J Med 1996;334:752–58
56. Miyata M, Smith JD. Apolipoprotein E allele-specific antioxidant activity and effects on cytotoxicity by oxidative insults and β-amyloid peptides. Nature Genet 1996;14:55–61

Received October 13, 2000
Revision received February 26, 2001
Accepted April 17, 2001